



Influence of processing route on electrical properties of $\text{Bi}_4\text{Ti}_3\text{O}_{12}$ ceramics obtained by tape-casting technology



M.G.A. Ranieri^{a,*}, E.C. Aguiar^{b,2}, M. Cilense^{b,2}, B.D. Stojanovic^c, A.Z. Simões^{a,1}, J.A. Varela^{b,2}

^a São Paulo State University, UNESP – Engineering Faculty, Guaratinguetá, SP 12516-410, Brazil

^b São Paulo State University, UNESP – Chemistry Institute, Araraquara, SP 14800-900, Brazil

^c Institute for Multidisciplinary Research, University of Belgrade, Kneza Viseslava 1, Belgrade, Serbia

ARTICLE INFO

Article history:

Received 24 July 2014

Received in revised form 25 February 2015

Accepted 29 March 2015

Available online 31 March 2015

Keywords:

A. Ceramics

B. Chemical synthesis

C. X-ray diffraction

ABSTRACT

Bismuth titanate powders ($\text{Bi}_4\text{Ti}_3\text{O}_{12}$ -BIT) were fabricated by solid state reaction (SSR) and polymeric precursor method (PPM). From these powders, $\text{Bi}_4\text{Ti}_3\text{O}_{12}$ pellets were obtained by tape-casting using plate-like templates particles prepared by a molten salt method. The BIT phase crystallizes in an orthorhombic structure type with space group *Fmmm*. Agglomeration of the particles, which affects the densification of the ceramic, electrical conduction and leakage current at high electric fields, was monitored by transmission electronic microscopy (TEM) analyses. FEG-SEM indicated that different shape of grains of BIT ceramics was influenced by the processing route. Both SSR and PPM methods lead to unsaturated *P*–*E* loops of BIT ceramics originating from the highly *c*-axis orientation and high conductivity which was affected by charge carriers flowing normally to the grain boundary of the crystal lattice.

© 2015 Published by Elsevier Ltd.

1. Introduction

Bismuth titanate ($\text{Bi}_4\text{Ti}_3\text{O}_{12}$) is a well-known member of the bismuth oxide layer structure ferroelectrics. It is a candidate for high-temperature piezoelectric applications, memory storage, and optical displays because of its high Curie temperature of 675 °C [1–3] and electrooptic switching behavior [4–13]. Its structure is formed by Bi_2O_2 layers separated by $\text{Bi}_2\text{Ti}_3\text{O}_{12}$ layer with orthorhombic structure at room temperature. Due to the fact that BIT is a lead free structure, it has attracted much attention in recent years [14,15]. The orthorhombic BIT unit possesses the lattice parameters of $a=0.5450$ nm, $b=0.54059$ nm, and $c=3.2832$ nm, and exhibits the spontaneous polarizations $P_s=50$ and $4\text{ }\mu\text{C}/\text{cm}^2$ along *a*- and *c*-axes, respectively [16]. The unit cell of this compound is orthorhombic allowing both 180° domain switching (switching along *a* axis) and 90° domain switching (interchanging of the *a* and *b* axes). In typical bismuth titanate textures arising from hot pressing or tape casting, the

possible polarization directions and ferroelastic distortions are aligned in a normal plane to the axis of crystal symmetry.

As the Bi_2O_3 increases leakage current, it is necessary to control its losses during thermal treatment by adding excess of bismuth due to the fact that its electrical properties such as remnant polarization, coercive field, dielectric permittivity and Curie temperature (T_c) are highly affected [17]. The main objective of the orientation engineering is to obtain *a*–*b* plane oriented BIT ceramics. It is also reported that the high electrical conductivity in the *a*–*b* plane makes poling difficult [18]. To obtain textured ceramics it is desired to align the grain growth and domains aiming to improve its mechanical, electrical, and ferroelectric properties following one specific direction [19]. Some techniques have been explored to fabricate textured ceramics including oriented grain growth and tape-casting. To obtain textured ceramics it is necessary to employ particles with anisotropic morphology (templates). These templates particles can be prepared by methods such as hydrothermal synthesis [20,21] and molten salt method [22–27].

Recently, efforts have been devoted to $\text{Bi}_4\text{Ti}_3\text{O}_{12}$ ceramics and thin films fabricated by various methods. The conventional ceramic route usually causes the non-stoichiometry, in consequence of the undesirable loss in bismuth content through volatilization of Bi_2O_3 at elevated temperature [28,29]. $\text{Bi}_4\text{Ti}_3\text{O}_{12}$ ceramics were conventionally prepared by solid-state reaction

* Corresponding author. Tel.: +55 12 3123 2765; fax: +55 12 3123 2800.
E-mail addresses: gabi.ranieri@ig.com.br (M.G.A. Ranieri), alezipo@yahoo.com (A.Z. Simões).

¹ Tel.: +55 12 3123 2765; fax: +55 12 3123 2800.

² Tel.: +55 16 3301 6643; fax: +55 16 3301 6692.

process, where oxide mixture of Bi_2O_3 and TiO_2 were ball milled, calcined at an intermediate temperature and finally sintered at high temperature. The conventional method requires a high calcination temperature, usually leading to inevitable particle coarsening and aggregation of the $\text{Bi}_4\text{Ti}_3\text{O}_{12}$ powders. However, using ball milling in high energy ball mills where the parameters as the ratio powdered-balls, speed and milling time are precisely determined, besides mechanical activation of initial powders and decreasing of its particle size, the mechanochemical reaction can occur [30]. Thus, solid state reaction as a result of induced mechanical and thermal energy during high energy milling could be rather easily initiated and the lower calcination and sintering temperature comparing to conventional solid state reaction would be required. Meanwhile, the problem of the hard particle agglomerate can be still present resulting in poor microstructure and properties of the $\text{Bi}_4\text{Ti}_3\text{O}_{12}$ ceramics. The novelty of present work in comparison with previous ones [4] is to evaluate the solid-state reactions initiated by intensive milling in high-energy ball mills as an alternative for the ceramic powder preparation. An important criterion for intensive milling is the formation of highly dispersed phased materials typical for metal powders or oxide based materials (mechanical activation) or the formation of new product because of a solid-state reaction (mechanochemical synthesis). Intensive milling increases the area of contact between the reactant powder particles due to reduction in particle size and allows fresh surfaces to come into contact. As a consequence, solid-state reactions that normally require high temperatures will occur at lower temperature during mechanochemical synthesis without any externally applied heat. In addition, the high defect densities induced by intensive milling in high-energy mills favor the diffusion process. Alternatively, the particle refinement and consequent reduction in diffusion distances (due to microstructural refinement) can at least reduce the reaction temperatures significantly, even if they do not occur at room temperature. Further, mechanical treatment of ceramic powders can reduce particle size and enable obtainment of nano-structured powders, which are of the main interest in current trend of miniaturization and integration of electronic components. On the other hand, polymeric precursor method, which originates from the method of Pechini, employs complexing of cations in an organic media, resulting in a homogeneous ion distribution at molecular level [15]. Because of the formation of a polyester resin during the synthesis, there is no segregation of cations during the thermal decomposition of organic matter. Hence, the main focus on this work is to prepare high-purity and anisotropic $\text{Bi}_3\text{Ti}_4\text{O}_{12}$ (BIT) based ceramics from different routes using BIT crystal as growth templates and by using these crystals evaluate the role of processing route on the phase formation, densification, grain orientation, textured microstructure and the electrical properties of the $\text{Bi}_4\text{Ti}_3\text{O}_{12}$ produced by tape casting technology.

2. Experimental

In this work, $\text{Bi}_4\text{Ti}_3\text{O}_{12}$ powders with 10 wt.% of bismuth excess were prepared by SSR and PPM methods. The 10 wt.% of bismuth excess was added to minimize bismuth loss during thermal treatment. Pure phase could not be obtained without additional bismuth, as reported in the literature [31]. The following reagents were employed to obtain BIT by solid state reaction: Bi_2O_3 (98.0%, Vetec), TiO_2 (98.5%, Labsynth), Na_2SO_4 (99.0%, Labsynth) and K_2SO_4 (99.0%, Labsynth). Mixture of Bi_2O_3 and TiO_2 in the equimolar ratio mechanochemically treated in a Fritsch Pulverisette 5 planetary ball mill. The zirconia oxide vial of 500 cm^3 charged with zirconia oxide balls of a nominal diameter of $\sim 10\text{ mm}$ were used as the milling medium. The primary mass of the powder mixture was 20 g; hence the ball-to-powder mass ratio was 20:1. The angular

velocity of the supporting disc and vials was 33.2 rad s^{-1} (317 rpm) and 41.5 rad s^{-1} (396 rpm), respectively. The powder was milled for 120 min. On the other hand, the BIT phase obtained by the polymeric precursor method employed the following reagents: $\text{Bi}(\text{NO}_3)_3 \cdot 5\text{H}_2\text{O}$ (100.1%, Mallinckrodt), $\text{Ti}(\text{OC}_3\text{H}_7)_4$ (97.0%, Alfa Aesar), $\text{C}_6\text{H}_8\text{O}_7 \cdot \text{H}_2\text{O}$ (99.5%, Merck), $\text{C}_2\text{H}_6\text{O}_2$ (99.7%, Synth), HNO_3 (99.9% Synth), $\text{C}_2\text{H}_8\text{N}_2$ (98.0%, Nuclear), NH_4OH (99.9%, Qhemis) and $\text{C}_2\text{H}_8\text{N}_2$ (99.8%, Aldrich).

$\text{Bi}_4\text{Ti}_3\text{O}_{12}$ templates were prepared by a molten-salt method according to Ref. [31]. Equal weight of $\text{Bi}_4\text{Ti}_3\text{O}_{12}$ powder and $\text{Na}_2\text{SO}_4/\text{K}_2\text{SO}_4$ eutectic mixture was mixed in a sealed alumina crucible and heated at 1000°C for 0.5 h. After cooling slowly to the room temperature, the reaction product was separated by centrifugation and washed several times with hot de-ionized water to remove the sulfate salts and then dried at 100°C . For slurry preparation, 10 vol.% $\text{Bi}_4\text{Ti}_3\text{O}_{12}$ powder was dispersed in de-ionized water using 1 wt.% (on the dry weight basis) acrylic acid as a dispersant (99%, Aldrich), and the pH value was adjusted to 9 with analytical grade ammonia (99.9%, Qhemis). During the milling, 5 wt.% (on the dry weight basis) polyvinyl alcohol (99.6%, Vetec) and 2.5 wt.% (on the dry weight basis) glycerin (99.5%, Cromoline) were added as a binder and a plasticizer, respectively. The slurry was mixed for 24 h. 5 wt.% $\text{Bi}_4\text{Ti}_3\text{O}_{12}$ platelets powder was added and mixed with the $\text{Bi}_4\text{Ti}_3\text{O}_{12}$ slurry under electromagnetic stirring for 4 h. Finally, the slurry was degassed under vacuum and tape casted on a glass surface at a speed of 0.5 cm/s and a single “doctor blade” with an aperture of $120\text{ }\mu\text{m}$. For polymeric precursor method, the tapes obtained were dried at room temperature, cut into pieces of 5 mm^2 , stacked and laminated at a pressure of 80 MPa for 10 min at 150°C . The binder and plasticizer were burned out at a temperature of 500°C for 3 h with a heating rate of 1°C/min . The laminates were then sintered in air in a sealed alumina crucible at 800°C . The tapes obtained by the solid state reaction were dried at room temperature, cut into pieces of 5 mm^2 , stacked and laminated at a pressure of 80 MPa for 5 min at 50°C . The laminates were then sintered in air at 1000°C , heating rate 5°C/min and level 4 h.

2.1. Characterization

Powders were first analyzed by X-ray diffraction (XRD) for phase determination. X-ray diffraction data were collected with a Rigaku 20-2000 diffractometer under the following experimental conditions: 40 kV , 30 mA , $20^\circ \leq 2\theta \leq 60^\circ$, $\Delta 2\theta = 0.02^\circ$, $\lambda_{\text{Cu K}\alpha}$ monochromatized by a graphite crystal, divergence slit = 2 mm , reception slit = 0.6 mm , step time = 10 s . Specimens for TEM were obtained by drying droplets of as-prepared samples from isopropyl alcohol dispersion which had been treated in ultrasonic bath for 5 min onto 300 mesh Cu grids. TEM images and patterns were then taken at an accelerating voltage of 200 kV on a Philips model CM 200 instrument. A FEG-SEM was used to analyze the morphology. Resistivity was determined by current–voltage in voltage source (KEITLEY 237-USA) coupled with high voltage meter, voltage ranging from 0 to 1100 V in pulsed mode. Ferroelectric properties of the capacitor were measured at room temperature using a Radiant Technology RT6000A in a virtual ground mode, respectively at 1 MHz . All measurements were taken at room temperature.

3. Results and discussion

The $\text{Bi}_4\text{Ti}_3\text{O}_{12}$ phase obtained by conventional SSR and by the PPM methods was monitored by XRD, Fig. 1(a) and (b). The diffraction pattern of the powders obtained by PPM shows intensive Bragg peaks and no impurities observed. On the other hand, Bragg peaks of the BIT phase obtained by the SSR are weaken

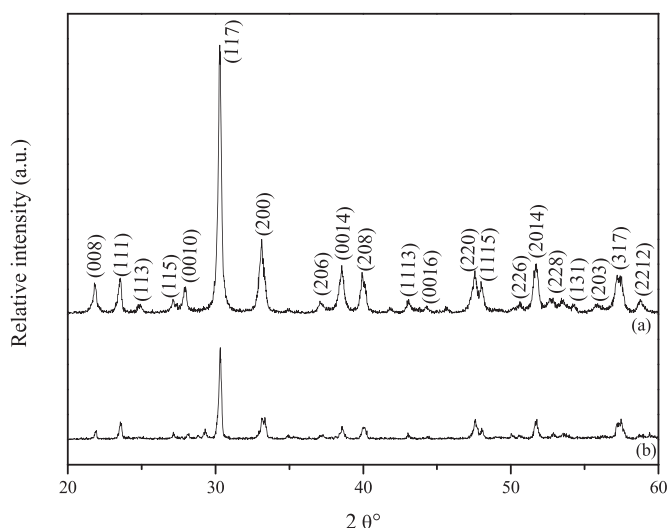


Fig. 1. X-ray diffraction patterns of BIT powders obtained by (a) PPM method and by (b) SSR.

and broad peaks are evident. This means that the PPM provides low calcination temperature to synthesize BIT. Bragg reflection peaks are indicative of perovskite structure, with orientation in *c*-plane, mainly characterized by higher intense peak (*hkl* – 117) and no apparent peak splitting is identified. Our XRD results are in agreement with those reported in the literature [32–35]. According to Stojanovic et al. [11], the BIT phase can be processed by the mixture of Bi_2O_3 and TiO_2 oxides milled for various times and mechanically activated in the high energy ball mill followed by mechanochemical reaction. The authors verified that only by homogenization of initial powders using conventional ball milling, the mechanical activation would not occur and did not trigger any reaction among mixed oxides and sharp peaks of crystalline Bi_2O_3 and TiO_2 could be still observed.

To analyze the morphology of the BIT powders, transmission electronic microscopy was used as shown in Fig. 2(a) and (b). It is necessary to note that the powder dissolved in acetone was de-agglomerate in ultrasonic bath before analysis. The images showed agglomerates that could not be destroyed in above mentioned process. Soft agglomerated powder is needed both for dry processing methods, e.g. powder compaction, and for the preparation of stable suspensions in liquids, e.g. for thin or thick film production. Unless weakly agglomerated nanoscale powders can be produced, the benefits expected from highly-uniform nanocrystalline powders are easily lost during the manufacture of components. The strength of agglomerates depends on the surface properties of the nanocrystalline particles and these properties are sensitively dependent on the powder synthesis [36]. SSR method reveals increased cluster agglomeration after calcinations of BIT powders which is indicative that longer time of milling (2 h) leads to a heterogeneous distribution of particles. BIT powders obtained by the PPM also reveal particle agglomeration. In this case, the high specific surface area of nanocrystalline powders provide a stronger tendency of the powder to agglomerate [36]. TEM images of bismuth titanate powders reveal that the specimens consist of nanocrystalline particles and no amorphous region was identified as in agreement with XRD study.

The diffraction pattern of the BIT pellets obtained by PPM and SSR methods with 5 wt.% of templates is shown in Fig. 3(a) and (b). Bismuth layered ferroelectrics are strongly anisotropic in nature with its ferroelectric properties being mostly influenced by the phase orientation [37]. Typical crystalline BIT phase is observed for the pellets obtained by SSR. The main peaks are oriented toward

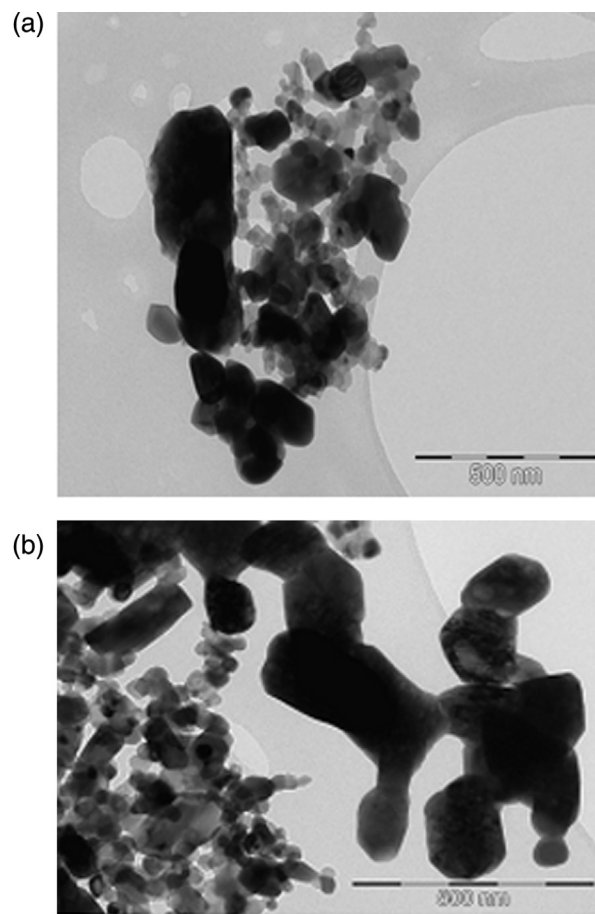


Fig. 2. Transmission electronic microscopy of BIT powders obtained by (a) PPM and by (b) SSR.

the *c*-axis (008), (0010), (0012), (117), (0014), (0016) and (0018) planes, as in agreement with literature data [1,2,31]. The system crystallizes in an orthorhombic crystal structure. There is a clear evidence that the main peaks are shifted to high $2\theta^\circ$ angles indicating that the templates do not act as simple crystal growth controller, which can avoid the interdiffusion between Bi_2O_3 and the main phase but also exhibit less intense (117) plane and a

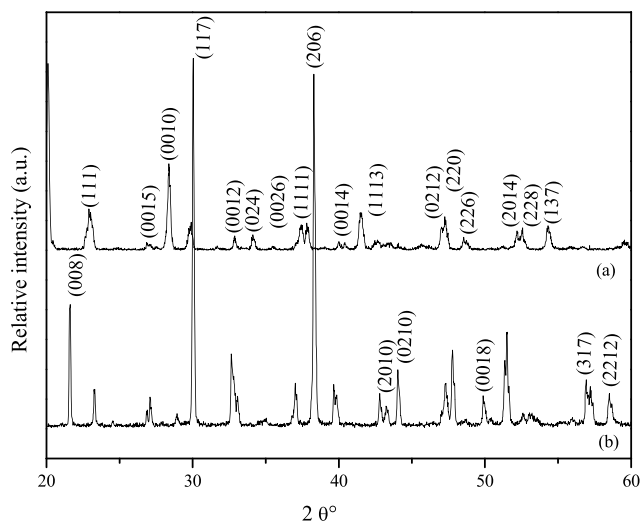


Fig. 3. X-ray diffraction patterns of BIT texture ceramic obtained by (a) PPM and by (b) SSR.

unstable phase at this temperature. Comparing both methods, the intensity of $\{001\}$ peaks in the sample obtained by SSR is enhanced in the direction perpendicular to tape-casting while the intensity of other peaks weakens. In contrast, the $\{hk0\}$ peaks enhance and the $\{hkl\}$ peaks weaken in the direction parallel to tape-casting, while the $\{001\}$ peaks become vanished. The results indicate that the ceramics obtained by PPM have obvious textured characteristics. It is well known that the seeds grow at the expense of fine-grained matrix particles during tape-casting. But once the fine-grained matrix particles are used up, the seeds will grow slowly and thus there is a slight increase in the degree of grain orientation. The origin of the texture development was partly attributed to the growth of template grains at the expense of small grains. Therefore, the growth of matrix grains as well as that of template grains is important to prepare highly textured ceramics by the tape-casting method.

The FEG-SEM images from BIT obtained by SSR and PPM methods are shown in Fig. 4(a) and (b). Elongated grains in the

form of platelets with homogeneous and packaged distribution that is a typical structure of bismuth with layered compounds Aurivillius type were observed by the PPM. According to Aguiar et al. [4] the SEM images of the randomly oriented samples exhibit mixed grain microstructures of equiaxed and platelike grains for BIT samples. The surface of the BIT pellets obtained by SSR was platelike with lengths ranging from 5 to 6 μm and a width of 1 μm while the surface of the pellet obtained by the PPM showed a rounded grains shape. The main reason for larger grains can be attributed to the interval of oxygen ion distribution along (006) with the BIT template which is closer to the a - and b -axes lattice parameters (0.541 nm) than that of the c -axis parameter (3.283 nm) of BIT. Also, changes in the shape and size of grains are a consequence of the high anisotropy of BIT templates which impact the process of formation and growth rate of each crystal face. BIT ceramics processed by PPM presented smaller grain sizes when compared to samples obtained by SSR. There is no evidence of liquid-phase segregated at the grain boundaries indicating that both routes allow obtaining the phase at low sintering temperature with particles distributed in a submetric matrix. Microstructures of textured BIT obtained by PPM which contained 5 wt.% template particles demonstrate that the bismuth titanate platelet grains are aligned in the casting direction and that the original platelets grew at the expense of fine matrix grains.

Fig. 5 shows the current–voltage behavior of bismuth titanate samples obtained by both methods. It is known that the BIT is a

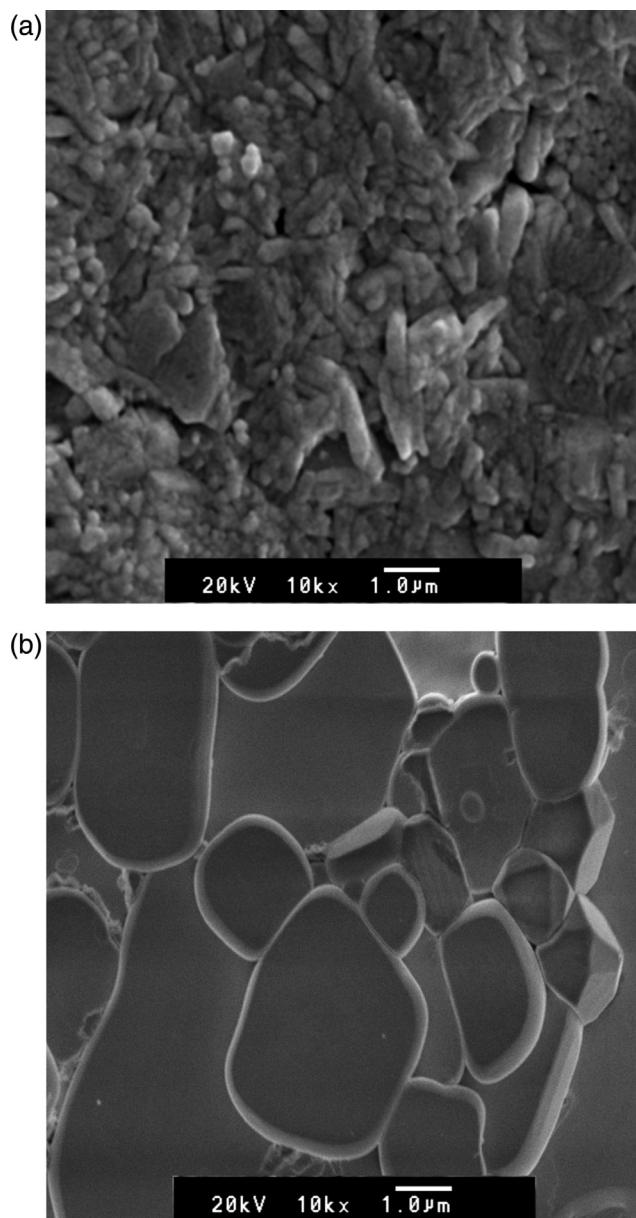


Fig. 4. FEG-SEM micrographies of BIT ceramics obtained by (a) PPM and by (b) SSR.

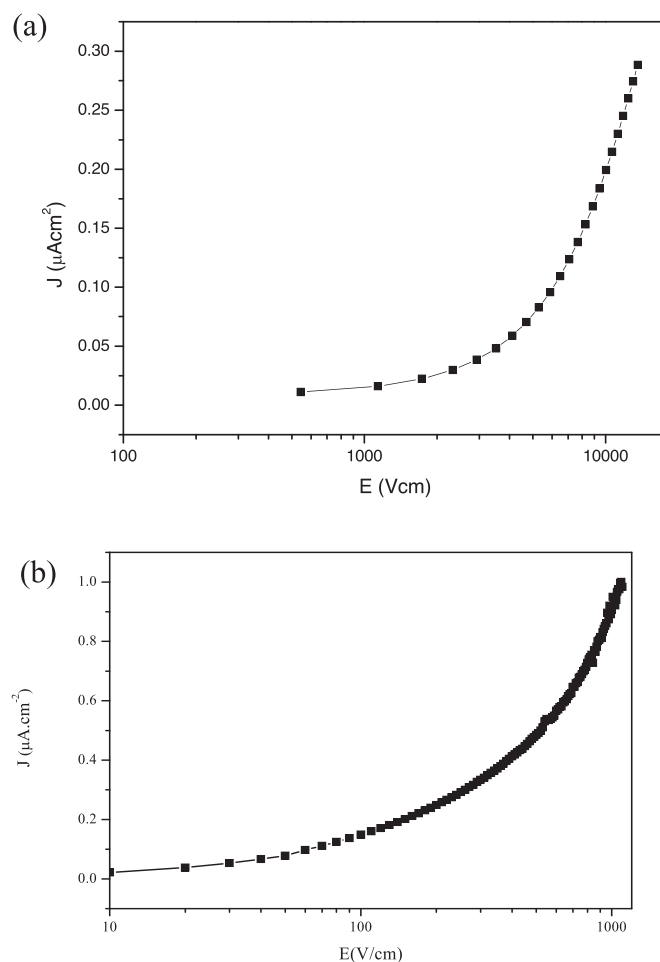


Fig. 5. Leakage current behavior as a function of electric field for bismuth titanate ceramics perpendicular (\perp) to the tape casting plane obtained by (a) PPM and by (b) SSR.

ceramic electronic conductivity of p-type. This present material mainly related to defects Bi^{3+} , according to the Eq. (1):



The above equation indicates that there are defects in the hole type ferroelectric materials. The leakage current density of the ferroelectric BIT pellet was influenced by the employed method. BIT ceramic obtained by the PPM shows low conductivity even when the applied electric field is high. The low conductivity can be attributed to textured ceramics that result in lower relative grain boundary allowing charge carriers to flow normally in the crystal lattice. In the plate-like structure observed in the PPM sample, carrier injection into the insulator looks very important, so space charge can distribute along the plate-like grain boundaries. On the other hand, BIT obtained by SSR has rounded shape grains which might have a lot of carrier traps. At the high electric field region, the localized carriers begin to come out of the trap, resulting in a large increase of current density. At low fields the leakage current density increased linearly with applied field implied ohmic characteristics. At high fields, these films exhibit nonlinear J – V relationships. The leakage density at 1000 V/cm was about $0.9 \mu\text{A}/\text{cm}^2$ and $0.03 \mu\text{A}/\text{cm}^2$, for the BIT pellets obtained by the solid state reaction and the polymeric precursor method, respectively. The competing effect between ethylenediamine and citric acid for the complexation of the bismuth ions makes more

pronounced the volumetric effect leading to rounded grain morphology of BIT obtained by the polymeric precursor method. This effectively reduces hydrogen number and symmetry of the molecule and the possibilities of a homogeneous interaction. The lower leakage current ($0.03 \mu\text{A}/\text{cm}^2$) observed for the pellet obtained by polymeric precursor method may be attributed to probable differences in grain size, density, surface structure and templates. The role of templates in this case is to increase the nucleation density and allows the consumption of oxygen vacancies by changing their oxygen nonstoichiometry and thus preventing or reducing accumulation of oxygen vacancies near the interface. This value is relatively reasonable for application in memories once a high leakage current generally leads to the loose of the stored data written in a cell and, thus, requires a frequent refresh and high power consumption [38].

The room-temperature polarization-electric field hysteresis loops of samples obtained by SSR and PPM are shown in Fig. 6. Hysteresis loops are not fully developed originating from a reduced polarizability along with the a -axis. This is a common result for polycrystalline bismuth-layered ferroelectrics, which exhibit a great polarization in a -axis direction, besides a smaller polarization along the c -axis and reflects the different orientation of the grains. It is difficult to align their polarization vector, so the total polarization in field direction is always moderate. Anisotropic remnant polarizations (P_r) and coercive fields (E_c) are observed in the sintered tapes perpendicular to the casting plane. These values are close to those previously reported for hot-forged bismuth titanate [39]. In bismuth titanate, the spontaneous polarization P_s lies in the monoclinic a – c plane at a small angle (4.5°) to the a -axis and exhibits two independently reversible components: $50 \mu\text{C}/\text{cm}^2$ along with the a -axis and $4 \mu\text{C}/\text{cm}^2$ along with the c -axis [40]. The small P_r of the BIT pellet obtained by the SSR originates from the highly c -axis orientation and high conductivity affecting charge carriers flowing normally to the grain boundary of the crystal lattice.

4. Conclusions

X-ray diffraction reveals the formation of $\text{Bi}_4\text{Ti}_3\text{O}_{12}$ powders by SSR and PPM methods which crystallize in an orthorhombic structure with space group $Fmmm$. The FEG-SEM micrographs of the randomly oriented samples exhibit mixed grain microstructures of equiaxed and platelike grains for PPM while for SSR rounded grain microstructure. Phase formation of BIT pellets evidenced obvious textured characteristics for the PPM indicating that the templates seeds grow at the expense of fine-grained matrix particles during tape-casting. The leakage current and the P – E loops of BIT pellets are strongly affected by grain morphology and the formation of highly textured microstructure in it. Further study is needed to investigate the piezoelectric properties of oriented thick films to make them compatible with silicon micromachining and thus more useful in practical applications.

Acknowledgements

The authors gratefully acknowledge to the financial support of the Brazilian financing agencies CNPq, FAPESP and SONY Corp. Research Center, Hodogaya-ku, Yokohama-shi 240, Japan.

References

- [1] Y. Kan, P. Wang, Y. Li, Y. Cheng, D. Yan, Fabrication of textured bismuth titanate by templated grain growth using aqueous tape casting, *J. Eur. Ceram. Soc.* 23 (2003) 2163–2169.
- [2] Z.Z. Lazaveric, N.Z. Romcevic, M. Todorovic, B.D. Stojanovic, Structural and ferroelectrical properties of bismuth titanate ceramic powders prepared by mechanically assisted synthesis, *Sci. Sinter.* 39 (2007) 177–184.

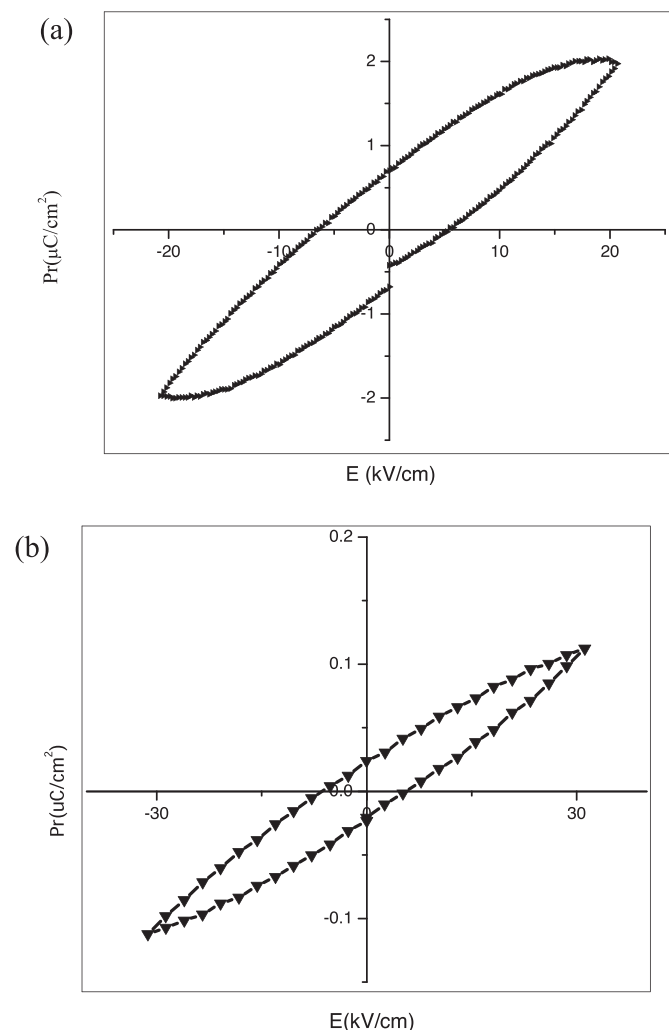


Fig. 6. P – E hysteresis loops of bismuth titanate textured perpendicular (\perp) to the tape casting plane obtained by (a) PPM and by (b) SSR.

- [3] M. Suzuki, Review on future ferroelectric nonvolatile memory: FeRAM, *J. Ceram. Soc. Jpn.* 103 (1995) 1088.
- [4] E.C. Aguiar, A.Z. Simões, C.R. Foschini, L.A. Perazolli, R.E. Mistler, E. Longo, J.A. Varela, Electrical properties of textured niobium-doped bismuth titanate ceramics, *J. Am. Ceram. Soc.* 95 (8) (2012) 2601–2607.
- [5] Y. Haixue, J. Reece, Effect of texture on dielectric properties and thermal depoling of $\text{Bi}_4\text{Ti}_3\text{O}_{12}$ ferroelectric ceramics, *J. Appl. Phys.* 100 (2006) 76–103.
- [6] J.A. Horn, S.C. Zhang, U. Selvaraj, G.L. Messing, S. Trolier-McKinstry, Templated grain growth of textured bismuth titanate, *J. Am. Ceram. Soc.* 82 (4) (1999) 921–926.
- [7] Q.-X. Bao, L.-H. Zhu, Q.-W. Huang, J. Xv, Preparation of texture $\text{Ba}_2\text{NaNb}_5\text{O}_{15}$ ceramics by templated grain growth, *Ceram. Int.* 32 (2006) 745–749.
- [8] S.S. Kim, J.-K. Chung, I.-S. Kim, J.-S. Song, C.J. Kim, W.-J. Kim, Dielectric properties of ferroelectric $(\text{Ba}_{0.6}\text{Sr}_{0.4})\text{TiO}_3$ thick films prepared by tape casting, *J. Electroceram.* 17 (2006) 451–454.
- [9] A. Sanson, R.W. Whatmore, Properties of $\text{Bi}_4\text{Ti}_3\text{O}_{12}$ – $(\text{Na}_{1/2}\text{Bi}_{1/2})\text{TiO}_3$ piezoelectric ceramics, *Jpn. J. Appl. Phys.* 41 (11) (2002) 7127.
- [10] L.B. Kong, J. Ma, W. Zhu, O.K. Tan, Preparation of $\text{Bi}_4\text{Ti}_3\text{O}_{12}$ ceramics via a high-energy ball milling process, *Mater. Lett.* 51 (2001) 108–114.
- [11] B.D. Stojanovic, C.O. Paiva-Santos, C. Jovalekic, A.Z. Simões, J.A. Varela, Mechanically activating formation of layered structured bismuth titanate, *Mater. Chem. Phys.* 96 (2006) 471–476.
- [12] V.K. Seth, W.A. Schulze, Grain-oriented fabrication of bismuth titanate ceramics and its electrical properties, *IEEE Trans. Ultrason. Ferroelectr. Freq. Control.* 36 (1989) 1.
- [13] Y. Kinemuchi, P.H. Xiang, H. Kaga, K. Watari, Preferred orientation of $\text{Bi}_4\text{Ti}_3\text{O}_{12}$ thick film, *J. Am. Ceram. Soc.* 90 (9) (2007) 2753–2758.
- [14] Z.S. Macedo, C.R. Ferrari, A.C. Hernandez, Impedance spectroscopy of $\text{Bi}_4\text{Ti}_3\text{O}_{12}$ ceramic produced by self-propagating high-temperature synthesis technique, *J. Eur. Ceram. Soc.* 24 (2004) 2567–2574.
- [15] W. Chen, Y. Hotta, T. Tamura, K. Miwa, K. Watari, Effect of section force and starting powders on microstructure of $\text{Bi}_4\text{Ti}_3\text{O}_{12}$ ceramics prepared by magnetic alignment via slip casting, *Scripta Mater.* 54 (2006) 2063–2068.
- [16] P.H. Xiang, Y. Kinemuchi, K. Watari, Preparation of axis-c-oriented $\text{Bi}_4\text{Ti}_3\text{O}_{12}$ thick films by template grain growth, *J. Eur. Ceram. Soc.* 27 (2007) 663–667.
- [17] D. Fu, T. Ogawa, T. Suzuki, K. Ishikawa, Thickness dependence of stress in lead titanate thin films deposited on Pt-coated Si, *Appl. Phys. Lett.* 77 (2000) 1532.
- [18] S. Kojima, R. Imaizumi, S. Hamazaki, M. Takashige, Raman scattering study of bismuth layer-structure ferroelectrics, *Jpn. J. Appl. Phys.* 33 (1995) 5559.
- [19] K. Shoji, Y. Uehara, Grain orientation of SbSI ceramics, *Jpn. J. Appl. Phys.* 30 (1) (1991) 2315–2317.
- [20] Y.B. Cheng, Q.B. Yang, Y.M. Kan, P.L. Wang, Y.X. Li, Q.R. Yin, D.S. Yan, Development of textured bismuth titanate piezoelectric ceramics, *Key Eng. Mater.* 247 (2003) 371–376.
- [21] X. Huiwen, K.J. Bowman, E.B. Slavovich, Hydrothermal synthesis of bismuth titanate powders, *J. Am. Ceram. Soc.* 86 (10) (2003) 1815–1817.
- [22] P.H. Xiang, Y. Kinemuchi, K. Watari, Preparation of c-axis-oriented $\text{Bi}_4\text{Ti}_3\text{O}_{12}$ thick films by template grain growth, *J. Eur. Ceram. Soc.* 27 (2–3) (2007) 663–667.
- [23] Q.W. Huang, J. Xu, L.H. Zhu, H. Gu, P.L. Wang, Molten salt synthesis of acicular $\text{Ba}_2\text{NaNb}_5\text{O}_{15}$ seed crystals, *J. Am. Ceram. Soc.* 88 (2) (2005) 447–449.
- [24] J. Xu, L.H. Zhu, Comparison of formation behavior of $\text{Ba}_2\text{NaNb}_5\text{O}_{15}$ in air and molten NaCl salt, *J. Mater. Sci.* 39 (10) (2004) 3445–3447.
- [25] T. Kimura, T. Kanazawa, T. Yamaguchi, Preparation of $\text{Bi}_4\text{Ti}_3\text{O}_{12}$ powders in the presence of molten salt containing LiCl, *J. Am. Ceram. Soc.* 66 (8) (1983) 597–600.
- [26] T. Motohashi, T. Kimura, Development of texture in $\text{Bi}_{0.5}\text{Na}_{0.5}\text{TiO}_3$ prepared by reactive-templated grain growth process, *J. Eur. Ceram. Soc.* 27 (13–15) (2007) 3633–3636.
- [27] Q.X. Bao, L.H. Zhu, Q.W. Huang, J. Xv, Preparation of textured $\text{Ba}_2\text{NaNb}_5\text{O}_{15}$ ceramics by templated grain growth, *Ceram. Int.* 32 (7) (2006) 745–749.
- [28] S.E. Cummings, L.E. Cross, Electrical and optical properties of ferroelectric $\text{Bi}_4\text{Ti}_3\text{O}_{12}$ single crystal, *J. Appl. Phys.* 39 (5) (1968) 2268–2274.
- [29] S. Kojima, A. Hushur, F. Jiang, S. Hamazaki, T. Takashige, M.S. Jang, S. Shimada, Crystallization of amorphous bismuth titanate, *J. Non-Cryst. Solids* 293–295 (2001) 250–254.
- [30] B.D. Stojanovic, A.Z. Simões, C. Quinelato, E. Longo, J.A. Varela, Effect of processing route on the phase formation and properties of $\text{Bi}_4\text{Ti}_3\text{O}_{12}$ ceramics, *Ceram. Int.* 32 (2006) 707–712.
- [31] M.G.A. Ranieri, E.C. Aguiar, M. Cilenese, A.Z. Simões, A.J. Varela, Syntheses of bismuth titanate templates obtained by the molten salt method, *Ceram. Int.* 39 (2013) 7291–7296.
- [32] B.D. Stojanovic, A.Z. Simões, C.O. Paiva-Santos, C. Quinelato, E. Longo, J.A. Varela, Effect of processing route on the phase formation and properties of $\text{Bi}_4\text{Ti}_3\text{O}_{12}$ ceramics, *Ceram. Int.* 32 (2006) 707–712.
- [33] Y. Kan, P. Wang, Y. Li, Y.B. Cheng, D. Yan, Low-temperature sintering of $\text{Bi}_4\text{Ti}_3\text{O}_{12}$ derived from a co-precipitation method, *Mater. Lett.* 56 (2002) 910–914.
- [34] M.E. Mendonza, F. Donado, J.L. Carrillo, Synthesis and characterization of micrometric ceramic powders for electro-rheological fluids, *J. Phys. Chem. Solids* 64 (2003) 2157–2161.
- [35] W.K. Chia, C.F. Yang, Y.C. Chen, The effect of Bi_2O_3 compensation during thermal treatment on the crystalline and electrical characteristics of bismuth titanate thin films, *Ceram. Int.* 34 (2008) 379–384.
- [36] A.Z. Simões, F.G. Garcia, C.S. Riccardi, Rietveld analysis and electrical properties of lanthanum doped BiFeO_3 ceramics, *Mater. Chem. Phys.* 116 (2009) 305–309.
- [37] R.R. Das, P.S. Dobal, A. Dixit, W. Pérez, M.S. Tomar, R.E. Melgarejo, R.S. Katiyar, Preparation and characterization of Ba and Nb substituted $\text{SrBi}_2\text{Ta}_2\text{O}_9$ compounds, *Mater. Res. Soc. Symp. Proc.* 655 (2001) CC5.6.1.
- [38] A.Z. Simões, A. Ries, F. Moura, C.S. Riccardi, E. Longo, J.A. Varela, Influence of the solution pH on the morphological, structural and electrical properties of $\text{Bi}_{3.50}\text{La}_{0.50}\text{Ti}_3\text{O}_{12}$ thin films obtained by the polymeric precursor method, *Mater. Lett.* 59 (2005) 2759–2764.
- [39] T. Takenaka, K. Sakada, Grain orientation and electrical properties of hot-forged $\text{Bi}_4\text{Ti}_3\text{O}_{12}$ ceramics, *Jpn. J. Appl. Phys.* 19 (1) (1980) 31–39.
- [40] S.E. Cummins, L.E. Cross, Electrical and optical properties of ferroelectric $\text{Bi}_4\text{Ti}_3\text{O}_{12}$ single crystals, *J. Appl. Phys.* 39 (5) (1968) 2268–2274.